Supplementary material for: Deterministic preparation of highly non-classical macroscopic quantum states

Ludovico Latmiral and Florian Mintert
QOLS, Blackett Laboratory, Imperial College London, London SW7 2AZ, United Kingdom
(Dated: August 20, 2018)

In this supplementary material, we provide an extensive discussion on the resilience of the state preparation to optical and mechanical decoherence, initial mechanical thermal noise and imperfect optical driving.

A. Perturbative regime

The Magnus expansion relies on the perturbative regime $k = \frac{g}{\omega_m} \ll 1$, and it is essential to gauge the range of applicability of the perturbative approximation. To this end, we compare the dynamics obtained with the Magnus expansion in third- and fourth-order approximation.
Applying the same procedure we have presented so far, we find the dynamics of the mirror after N mechanical periods at fourth order

$$V_m^{(4)}(N) = e^{-\frac{\pi}{3} i\ Nk^3\eta^2 Q_m}\ e^{-i\frac{\zeta^{(4)}}{2}(b^{\dagger 2}+b^2)^2} \times e^{i\pi k^4\eta^2\ N\left[\frac{124\eta-5}{20}(b^2+b^{\dagger 2})+\frac{575+634\eta}{90}b^\dagger b\right]}\ , \tag{S1}$$

with $\zeta^{(4)} = (\pi k^2\eta)^2 N\cot(\pi/N)$. Hence, we recall an important figure of merit, *i.e.* the state fidelity between two quantum states ϱ_A and ϱ_B, which is defined as

$$\mathcal{F}_{A,B} = \left(\mathrm{Tr}\sqrt{\varrho_A^{1/2}\varrho_B\varrho_A^{1/2}}\right)^2 . \tag{S2}$$

This quantity can be used to provide an estimate of the accuracy of the state preparation computed at the third order in Magnus, ϱ_3, by comparing it with ϱ_4, obtained by numerically propagating Eq.(S1). Fig. S1 depicts $\mathcal{F}_{3,4}$ as function of the driving time in terms of mechanical periods. We infer that the deviations between ϱ_3 and ϱ_4 are in the permille regime for the first 10 driving periods, and even at $N = 20$, the third order approximation is accurate within $\simeq 1\%$. We deem an error of 1% below the accuracy of what could be achieved experimentally within the next years, and thus feel that the perturbative treatment is highly adequate for the present purpose.

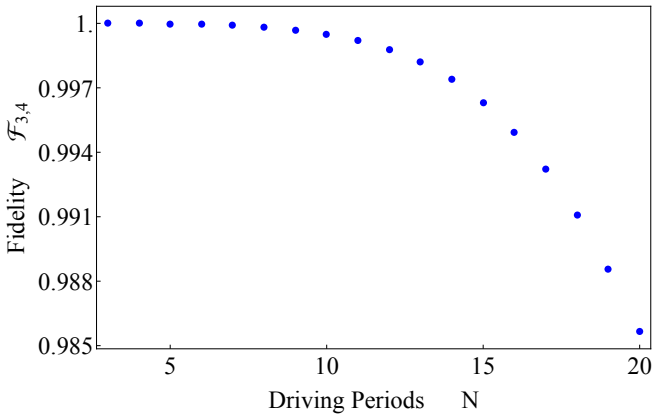

FIG. S1: Fidelity between the state of the mirror computed via a third and a fourth order Magnus expansion as a function of the integration time, expressed in terms of mechanical driving periods. The experimental parameters are set as $\eta = 20$, $k = 1/60$. The graph indicates that high fidelity is obtained up to 20 driving periods: $\mathcal{F}_{3,4} \gtrsim 0.985$.

B. Experimental imperfections

It is appropriate to gauge how unavoidable experimental imperfections will affect the desired process. To this end, we analyse the impact of optical and mechanical decoherence, initial thermal excitations in the mirror and imperfect phase shifts of the driving fields. Since the dynamics takes place in a high-dimensional Hilbert spaces of both mechanical and optical degree of freedom, this discussion is necessarily restricted to approximate methods. Together with the verification of the quality of the perturbative expansion (discussed in B 1 below), this seems adequate to estimate the order of magnitude of imperfections.

1. *Optical decoherence*

Due to experimental difficulties, the most delicate aspect affecting the unitarity of the evolution, and consequently the preparation of the desired mechanical state, is attributable to optical losses. The leakage of photons from the cavity is quantified by the decay rate κ, which is defined as the inverse of the time light remains in the cavity. A common approach to include the effects of such photon losses in the dynamics is to express the evolution of the system density matrix ρ in terms of the Master equation $\dot\rho = -i\,[H,\rho] + \kappa\mathcal{L}_a[\rho]$, where H is the system Hamiltonian and $\mathcal{L}_a[\rho]$ is the Lindblad operator $\mathcal{L}_a[\rho] = (a\rho a^\dagger - \{a^\dagger a,\rho\}/2)$.
When operating in the so called *resolved sideband* regime with $\kappa \ll \omega_m$, that is realised in many current experiments [1–4], the impact of photon loss can be captured by looking at the perturbative solution of the Master equation. To this end, we consider the Master equation for $\tilde\rho = V^\dagger(t)\rho V(t)$, where $V(t)$ satisfies $i\dot V = HV$, as

obtained in the main text (see Eq.6).

Solving this perturbatively, yields the contribution of photon loss to the dynamics in terms of powers of κ/ω_m. The integration for a generic time t assumes a rather complex form and correlations between field and mirror are created because of dissipation. However, thanks to the very specific bi-chromatic driving pattern many terms cancel out at the end of the evolution. Actually, our proposed set of constant phase shifts $\{\varphi_k\}$ is crucial to suppress the majority of these unwanted non-unitary and de-coherent contributions, including all correlation terms proportional to the driving amplitude η.

More specifically, in leading order in k and κ, we obtain at $t = \mathrm{NT}$ an expression that is completely independent of η and is thus well suited to describe the strong driving regime

$$\tilde{\rho}(NT) \simeq \tilde{\rho}(0) + \kappa NT \left(\tilde{a}\tilde{\rho}\tilde{a}^\dagger - \frac{1}{2}\{\tilde{a}^\dagger\tilde{a}, \tilde{\rho}\} \right) , \qquad \text{(S3)}$$

with

$$\tilde{a} = a e^{\frac{g}{\omega_m}(b-b^\dagger)} . \qquad \text{(S4)}$$

This result has a very clear physical interpretation: since the light-matter interaction conditionally displaces the mirror by an amount proportional to the number of photons in the cavity, each photon that has leaked out of the resonator should then be matched with a *missing* displacement $e^{g(b-b^\dagger)/\omega_m}$ of the mirror as indicated in Eq.(S4).

Fig.S2 depicts the state fidelity (see Eq.(S2)) after $N = 20$ mechanical periods as a function of the ratio κ/ω_m between the full state of the system (cavity plus mirror) obtained in the leaking scenario in Eq.(S3) and the ideal one discussed in the main text. As one can see, a loss rate satisfying $\kappa/\omega_m < 10^{-2}$ results in a reduction of the fidelity by $\lesssim 3\%$. This condition, together with the strong driving regime, is in accordance with Ref.[5],

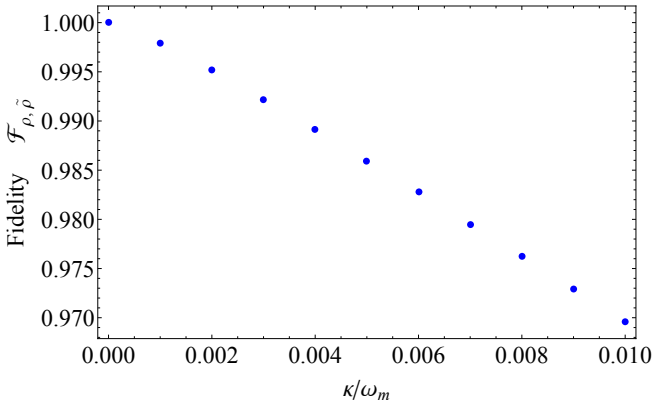

FIG. S2: Fidelity between the final state of the system (cavity plus mirror) in case of photon losses and the ideal scenario as a function of the cavity decay rate κ for an evolution lasting 20 mechanical periods.

where the resolved sideband regime and the condition $g/\kappa > 1$ were theoretically derived as requirements to resolve the *granularity* of the photon stream and fully exploit the non-linearity of the system to observe purely quantum features.

2. *Thermal initial state of the mirror*

Since the evolution operator V (see Eq.6 of the main text) factorises into a propagator for the mirror and a propagator for the cavity, one obtains a product state of mirror and cavity for any initial product state. That is, there is no fundamental need to require the mirror to be initially cooled exactly to the ground state, but initial thermal excitation of the mirror will affect the non-classicality of the final state.

Fig.S3 depicts cuts through the Wigner function of the mirror after 20 periods of driving for different initial thermal populations with $\langle n_m^{th}\rangle = 1$ and $\langle n_m^{th}\rangle = 10$, *i.e.* above the experimental threshold of $\langle n_m^{th}\rangle \sim 0.2$ achievable with sideband cooling (at a mechanical frequency $\omega_m = 2\pi \times 10^7$Hz) [2, 6]. The strong oscillatory behaviour with negative values of W is clearly displayed for an initial state with $\langle n_m^{th}\rangle = 1$. Only for $\langle n_m^{th}\rangle = 10$, *i.e.* substantially above the limits of side-band cooling, the quantum mechanical features are mostly outshined by the thermal contributions.

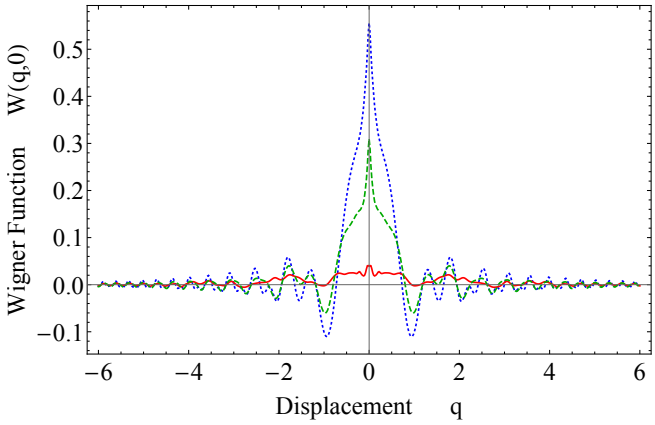

FIG. S3: Comparison of the cut profiles $p = 0$ of the Wigner function of the state of the mirror after an evolution lasting 20 mechanical periods with the mirror initially in its ground state (blue dotted line) and two thermal states with respectively $\langle n_m^{th}\rangle \sim 1$ (green dashed line) and $\langle n_m^{th}\rangle \sim 10$ (red line). The experimental parameters are set as $\eta = 20$, $k = 1/60$ and $\omega_m = 2\pi \times 10^7$Hz.

3. *Mechanical decoherence*

The main source of mechanical decoherence for a cooled optomechanical resonator arises from mechanical damping, which is characterised by the rate γ_m at which

a phonon excitation is lost in the environment. In case of non-zero temperature, however, the unwanted absorption of thermal excitations should also be taken into account. The process is conceptually analogous to optical photon losses from the cavity which happen at rate κ. Current experiments have achieved mechanical damping substantially below photon loss ($\gamma_m \ll \kappa$), what suggests that mechanical decoherence will not be a limiting factor. Since, however, highly non-classical, coherent superpositions of macroscopically distinct states are particularly sensitive to decoherence, a critical assessment of motional decoherence is in order. To this end we analyse the dynamics induced by the Master equation $\dot{\rho} = -i[H,\rho] + \gamma_m[(\langle n_m^{th}\rangle + 1)\mathcal{L}_b[\rho] + \langle n_m^{th}\rangle \mathcal{L}_{b^\dagger}[\rho]]$, where $\mathcal{L}_b$ and $\mathcal{L}_{b^\dagger}$ are the Lindblad operators for phonon absorption and emission, defined similarly to Sec. B 1. Thanks to high mechanical quality factors $Q = \omega_m/\gamma_m \gg 1$ being achieved in various experimental realizations, a perturbative solution of the Master equation provided reliable estimates. At the end of the state preparation, the system state $\tilde{\rho}$ in the frame defined by $V(t)$ (defined in Sec. B 1) at leading order in γ_m and κ reads

$$\tilde{\rho}(NT) = \tilde{\rho}(0) + \gamma_m \left[(\langle n_m^{th}\rangle + 1)\mathcal{L}_m[\tilde{b},\rho] + \langle n_m^{th}\rangle \mathcal{L}_m[\tilde{b^\dagger},\rho]\right], \tag{S5}$$

with

$$\tilde{b} = b - \kappa(a^\dagger a + \frac{\eta^2}{2}) \, . \tag{S6}$$

The result is compact, as satisfactorily, many terms get simplified at the end of the evolution because of the very specific choice of the driving profiles. Fig.S4 depicts the state fidelity after $N = 20$ periods of driving as a function of Q^{-1}, both in the case of a zero-temperature environment (in blue) and for a thermal state with $\langle n_m^{th}\rangle \sim 1$ (red), as obtained in recent experiments [2, 6]. In both cases the impact of mechanical damping on the state fidelity is smaller than in the case of optical decoherence. In particular at zero temperature the impact is almost negligible (within the per-mille regime) and even with thermal noise, reductions of the fidelity are limited to a few percent.

4. *Optical and mechanical decoherence*

After having analyzed mechanical and optical decoherence separately, we finally assess their combined impact on state preparation in a non-perturbative analysis. To this end, we numerically solve the full master equation for mirror and cavity for the whole driving time interval, which is necessarily limited to a finite (low) dimensional subspace. We performed our numerical simulations truncating the cavity field and the mirror respectively to 15 and 35 excitations. This lower truncation of the Hilbert space restricts the range of safely explorable mechanical states to the subset $\langle n_m\rangle \lesssim 5$, which, leaving all others parameters unchanged, requires to account for smaller couplings (we have chosen $k = 1/90$).

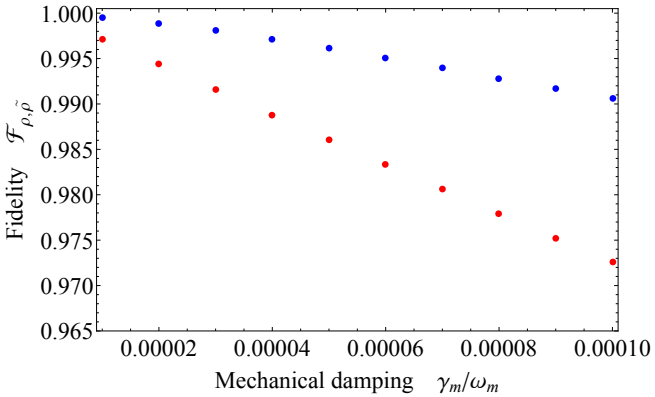

FIG. S4: Fidelity between the final state of the system (cavity plus mirror) in case of a mechanical damped evolution and the ideal scenario as a function of the mechanical damping γ_m/ω_m. Blue points are referred to the zero bath temperature case, while red points to $\langle n_m^{th}\rangle \sim 1$. The total evolution is supposed to last 20 mechanical periods with the mirror initially in its ground state and the dimensionless driving and coupling respectively set as $\eta = 20$ and $k = 1/60$.

We summarize in Fig.S5 the fidelity of the states obtained with a numerical solution of the full master equation accounting for photon losses and phonons absorption and dissipation. Results are in line with analytical discussions provided in Secs. B 1 and B 3. The overall reduction of fidelity remains in the percent regime, consistent with the above perturbative results.

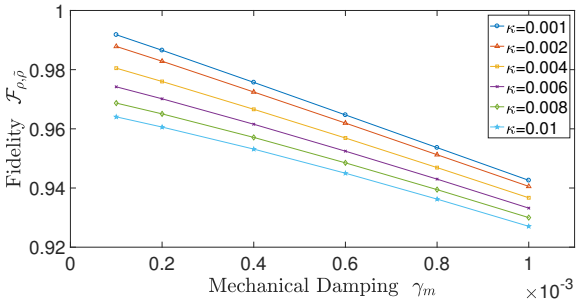

FIG. S5: Fidelity between the final state of the system (cavity plus mirror), obtained from a numerical simulation of the full master equation, as a function of the mechanical damping γ_m/ω_m and the optical decay rate κ. We assumed a cooled mechanical oscillator with a thermal bath at $\langle n_m^{th}\rangle \sim 1$. The total evolution is supposed to last 20 mechanical periods, the dimensionless driving and coupling are set to $\eta = 20$ and $k = 1/90$.

5. Laser driving

The central goal of deterministic state preparation is achieved through the application of appropriate phase shifts after each period of driving. Their experimental implementation seems feasible, since the shifts need to be applied on a time-scale that is short as compared to the inverse mechanical frequency. With $\omega_m \sim 10^6 s^{-1}$, this is orders of magnitude smaller than the optical characteristic frequency. Accurate control of optical phase has already been demonstrated in Ref.[7], where phase shift resolutions smaller than $\Delta\varphi = 10$mrad were achieved. The technique is based on high-speed fiber optical switchers with switching rate shorter than 1ns, which are already commercially available [8].

Still, despite the relative simplicity of such scheme, we deem it useful to consider the impact of deviations from the ideal driving profiles with the step-like phase shifts $\varphi_s = \frac{2\pi}{N}(s-1)$. To this end, let us replace the discontinuously evolving phase $\varphi(t) = \frac{2\pi}{N}\sum_s \Theta(t - sT)$ with the continuous function

$$\varphi_c^{(d)}(t) = \frac{2\pi}{N}\frac{t}{T} + \sum_{l=1}^{d} \varphi_l(t) \ ,$$

where $\frac{2\pi}{N}\frac{t}{T}$ is a linearly increasing phase factor and each term $\varphi_l(t) = A_l \sin(l\omega_m t)$ oscillates with frequency $l\omega_m$ and amplitude A_l. The set of amplitudes is chosen such that at any order d, $\varphi_c^{(d)}(t)$ is tangent to the step function in the centre of the step, *i.e.* for $t = (2j\pi + 1)/\omega_m$ with $j \in [0, N-1]$ (see Fig.S6 for a graphical representation).

Thanks to the continuous time dependance, it is then possible to analytically compute the generator with a Magnus expansion over the entire time window $t = NT$, and subsequently numerically integrate the dynamics over N mechanical periods. Interestingly, we obtain a separable propagator at every order d, without correlations between mirror and cavity, and which will still result in deterministic state preparation.

Most importantly, while resorting to the sole linear function $\frac{2\pi}{N}\frac{t}{T}$ single-particle terms of the cavity do not completely cancel out, resulting in a final average population $\langle n_c\rangle \sim 0.2\langle n_m\rangle$, these contributions are efficiently suppressed already at the order $d = 3$, when $\langle n_c\rangle \sim O(10^{-7})\langle n_m\rangle$ (see Fig.S6). This is an essential requirement since cavity excitations could potentially prevent the final readout through *back-action-evading* interaction.

Remarkably, the final non-classical mechanical state of the mirror obtained with these imperfect driving pattern presents a very high fidelity $\mathcal{F} \simeq 0.98$ with the ideal step-like case.

C. Readout

The final readout of the mechanical motion is a matter that has already been widely analysed theoretically [9, 10] and implemented experimentally [6, 11] with high precision. The most promising technique to perform quantum state reconstruction is called *back-action-evading* interaction and is based on state transfer. When the mirror is in the state of interest and the cavity is empty, a red detuned laser with frequency $\omega_d = \omega_c - \omega_m$ induces exchange of excitations from the former to the latter. Hence, tomography of the prepared mechanical state of the mirror can be carried out through homodyne measurement of the light leaking out of the cavity [12, 13].

Since we ensure that there are no residual correlations between cavity and mirror when the measurement protocol is applied, the desired mechanical quantum state is deterministically read out.

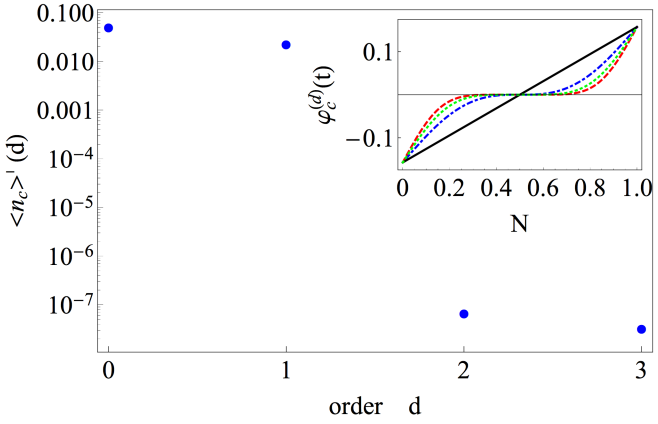

FIG. S6: Cavity occupation renormalized with respect to the population of the mirror $\langle n_c\rangle' = \langle n_c\rangle/\langle n_m\rangle$ as a function of the order of the decomposition of the step function d. In the top-right corner we plot an enlargement of the driving profiles defined by $\varphi_c^{(d)}(t)$ over the first mechanical period: linear approximation with $d = 0$ (black line), $d = 1$ (blue dashed-dotted), $d = 2$ (green dotted) and $d = 3$ (red dashed). The experimental parameters are set as $\eta = 20$, $k = 1/60$, $N = 20$.

[1] Thompson, J. D. *et al.* Strong dispersive coupling of a high-finesse cavity to a micromechanical membrane. *Nature* **452**, 72 (2008).

[2] Teufel, J. D. *et al.* Sideband cooling of micromechanical motion to the quantum ground state. *Nature* **475**, 359 (2011).

[3] Aspelmeyer, M., Kippenberg, T. J. & Marquardt, F. Cavity optomechanics. *Rev. Mod. Phys.* **86**, 1391 (2014).

[4] Wollman, E. E. *et al.* Quantum squeezing of motion in a mechanical resonator. *Science* **349**, 952 (2015).

[5] Miao, H., Danilishin, S., Corbitt, T. & Chen, Y. Standard quantum limit for probing mechanical energy quantization. *Phys. Rev. Lett.* **103**, 100402 (2009).

[6] Clark, J. B., Lecocq, F., Simmonds, R. W., Aumentado, J. & Teufel, J. D. Sideband cooling beyond the quantum backaction limit with squeezed light. *Nature* **541**, 191 (2017).

[7] Thom, J., Wilpers, G., Riis, E. & Sinclair, A. G. Accurate and agile digital control of optical phase, amplitude and frequency for coherent atomic manipulation of atomic systems. *Opt. Express* **21**, 18712 (2013).

[8] URL `https://www.thorlabs.com/`.

[9] Zhang, J., Peng, K. & Braunstein, S. L. Quantum-state transfer from light to macroscopic oscillators. *Phys. Rev. A* **68**, 013808 (2003).

[10] Vanner, M. R., Pikovski, I. & Kim, M. S. Towards optomechanical quantum state reconstruction of mechanical motion. *Ann. Phys.* **527**, 15 (2015).

[11] Lei, C. U. *et al.* Quantum nondemolition measurement of a quantum squeezed state beyond the 3 db limit. *Phys. Rev. Lett.* **117**, 100801 (2016).

[12] Smithey, D. T., Beck, M., Raymer, M. G. & Faridani, A. Measurement of the wigner distribution and the density matrix of a light mode using optical homodyne tomography: Application to squeezed states and the vacuum. *Phys. Rev. Lett.* **70**, 1244 (1993).

[13] D'Ariano, G. M., Macchiavello, C. & Paris, M. G. A. Detection of the density matrix through optical homodyne tomography without filtered back projection. *Phys. Rev. A* **50**, 4298 (1994).